Nano Energy 98 (2022) 107332

Contents lists available at ScienceDirect

Nano Energy

journal homepage: www.elsevier.com/locate/nanoen

The continuous efficient conversion and directional deposition of lithium (poly)sulfides enabled by bimetallic site regulation

Cheng Zhou [a,1], Minjie Chen [b,1], Chenxu Dong [c], Hong Wang [d], Chunli Shen [a], Xiuxiu Wu [a], Qinyou An [a], Ganggang Chang [b,*], Xu Xu [a,c,**], Liqiang Mai [a,e,**]

[a] State Key Laboratory of Advanced Technology for Materials Synthesis and Processing, Wuhan University of Technology, Wuhan 430070, Hubei, PR China
[b] School of Chemistry, Chemical Engineering and Life Science, Wuhan University of Technology, Wuhan 430070, Hubei, PR China
[c] International School of Materials Science and Engineering, Wuhan University of Technology, Wuhan 430070, Hubei, PR China
[d] Nanostructure Research Center (NRC), Wuhan University of Technology, Wuhan 430070, Hubei, PR China
[e] Foshan Xianhu Laboratory of the Advanced Energy Science and Technology Guangdong Laboratory, Xianhu Hydrogen Valley, Foshan 528200, Guangdong, PR China

ARTICLE INFO

Keywords:
Lithium (poly)sulfides
Continuous adsorption and catalysis
Directional deposition
2D metal-organic frameworks
Separator

ABSTRACT

The shuttle effect caused by the dissolution and accumulation of soluble (poly)sulfides seriously affects the reaction process and cycle performance of the lithium sulfur (Li-S) battery. One of the most effective strategies is the separator modification. The adsorption and catalytic mechanism of separator modification layer will cause discontinuous polysulfide conversion and loss of active substances. Therefore, 2D-bimetallic centered Zn/Co-ZIF nanosheets prepared by a novel method are selected to settle this unsolved problem for the first time. By regulating the metal center sites, the ability of ZIF nanosheets to transform (poly)sulfides is greatly improved. Further, based on the difference in conductivity between the ZIF modification layer and the cathode, the continuous efficient conversion and directional deposition of lithium (poly)sulfides to the cathode are realized. The battery assembled with the functional separator can deliver an initial capacity of up to 1304 mAh g^{-1} at 0.5 C, and excellent rate performance of 788 mAh g^{-1} at 3 C. Even at the current density of 2 C, the capacity attenuation rate of 1000 cycles is only 0.025% per cycle. This work will greatly promote the preparation of MOF materials and their application in Li-S batteries, and will further provide a new idea for the modification layer and cathode design.

1. Introduction

Due to the high theoretical capacity (1675 mAh g^{-1}) and energy density (2600 Wh kg^{-1}), lithium sulfur (Li-S) battery is considered to be the most potential next generation energy storage system for developing high-performance electric vehicles or even large-scale energy storage power stations [1,2]. However, the development of Li-S battery is limited by a series of problems, including poor conductivity of sulfur, volume expansion and shuttle effect [3,4]. After decades of research, it is found that the simple carbon sulfur composite cathode can well solve the problems of volume expansion and poor conductivity of sulfur cathode, while the shuttle effect can not be effectively suppressed [5,6]. Further introducing polar materials into the cathode to chemically adsorb (poly) sulfides will inevitably reduce the content of active substances in the cathode and lose the advantage of high energy density of Li-S battery [7–10].

The separator is an important part of the battery, which plays a role in blocking electrons and ensuring effective ion transport. At present, the most commonly used separator is the commercial polyolefin-based separator, which mainly ensures the transmission of lithium ions through micro-sized pores. For Li-S battery, the soluble polysulfide produced during the charge-discharge processes will inevitably shuttle through the pores, resulting in the loss of active substances and adverse side reactions, and finally leading to the reduction of Coulombic efficiency and the rapid attenuation of capacity. Therefore, the modification of the separator is of great significance to improve the cycle stability of

* Corresponding author.
** Corresponding authors at: State Key Laboratory of Advanced Technology for Materials Synthesis and Processing, Wuhan University of Technology, Wuhan 430070, Hubei, PR China.
E-mail addresses: changgang2016@whut.edu.cn (G. Chang), xuxu@whut.edu.cn (X. Xu), mlq518@whut.edu.cn (L. Mai).
[1] These authors contributed equally to this work.

https://doi.org/10.1016/j.nanoen.2022.107332
Received 18 March 2022; Received in revised form 21 April 2022; Accepted 28 April 2022
Available online 3 May 2022

the Li-S battery [11,12]. In recent years, since the separator modification will not affect the sulfur content of the cathode, from the initial carbon materials (porous carbon, carbon nanotubes, graphene oxide, et al.) to the subsequent polar materials (transition metal compounds, metal organic frameworks, et al.), a large number of different materials have been used to modify the separator of Li-S battery, and some exciting results have been achieved [13–15].

At present, in addition to the simplest barrier effect of (poly)sulfides, the explanation of the mechanism of separator modification layer mainly focuses on adsorption or catalysis [16–18]. Single adsorption or catalysis can not effectively inhibit the shuttle effect, because the adsorption capacity of the material for (poly)sulfides is limited and catalysis also requires adsorption of (poly)sulfides to active sites. In detail, if the soluble (poly)sulfides can not be quickly transformed into insoluble short chain (poly)sulfides and deposited on the cathode again, the active sites on the separator will be occupied, which will also cause the loss of active substances and the role of the modification layer will be greatly reduced. On the other hand, if the adsorption effect of the material on (poly)sulfides is weak, the (poly)sulfides cannot be in full contact with the catalytic sites, so as to give full play to the catalytic effect of the material. If the adsorption effect of the material for (poly) sulfides is too strong, the (poly)sulfides will be limited in the modification layer and reduce the utilization rate of active substances. Therefore, how to balance the relationship between adsorption and catalysis to realize continuous efficient conversion and directional deposition of lithium (poly)sulfides to the cathode is of great significance. At present, there are some studies on the adsorption and catalytic effects of cathode host [19–25], but there is no systematic study on the adsorption and catalysis of (poly)sulfides by separator modification layer. Sun et al. constructed a CoB_2 modified PP separator [26]. Due to the high density of adsorption sites and synergistic adsorption, the Li-S battery assembled with the modified separator showed good cycle stability and rate performance. Wang et al. employed Co-N-C as the modification layer [27]. The composite structure can effectively block (poly)sulfides and promote their transformation to short chains. Although these works have achieved good results, they have not passed relevant tests to prove that the materials do play a catalytic role. Therefore, exploring and obtaining the mechanism is of great significance for the selection of separator modification layer materials. As far as we know, consist of metal ions and organic ligands, MOFs possess both adsorption and catalytic activities to (poly)sulfides [28–32]. By further regulating its structure, such as manufacturing defects, adjustment of metal center, the synergistic effect of adsorption and catalysis can be effectively changed [33–38].

2. Result and discussion

2.1. DFT calculation and reaction mechanism

Herein, the two-dimensional bimetallic Zn/Co-ZIF nanosheet is selected as the object to systematically study the relationship between the adsorption and catalysis of (poly)sulfides in the separator modification layer. (Fig. 1a). Firstly, the catalytic and adsorption effects of pure ZIF-67 (Co) and pure ZIF-8 (Zn) on different kinds of (poly)sulfides and S_8 (Fig. S1) are verified by DFT calculations. Fig. 1b shows the calculated Gibbs free energy required for the conversion of each polysulfide for ZIF-8 and ZIF-67, respectively. It can be seen that the Gibbs free energies of ZIF-67 are significantly lower than that of ZIF-8. Especially for the speed-limiting step (from Li_2S_4 to Li_2S_2) of the whole conversion process, the Gibbs free energy of ZIF-67 is 1.72 eV, which is much lower than that of ZIF-8 (3.30 eV). This result shows that ZIF-67 with Co metal center possess a better catalytic effect on (poly)sulfides and can promote the rapid conversion of (poly)sulfides. Furthermore, the binding energies of ZIF-8 and ZIF-67 for different (poly)sulfides are calculated respectively (Fig. 1c, Figs. S2,3). It can be seen that ZIF-8 posscess higher binding energy for soluble long-chain (poly)sulfides, indicating that ZIF-8 with Zn metal center can adsorb (poly)sulfides more effectively. On the one hand, this result shows that Zn and Co metal centers are conducive to the adsorption and catalysis of (poly)sulfides respectively, and it also shows that ZIF of Zn or Co metal centers alone can not effectively limit and convert (poly)sulfides. Therefore, by regulating the proportion of Zn and Co metal center sites in Zn/Co-ZIF, it is expected to achieve the synergistic effect of adsorption and catalysis for (poly) sulfides.

Compared to rGO host in the cathode, ZIF shows poor conductivity. As a result, after the soluble polysulfide is catalyzed at the interface between the cathode and the separator modification layer, the short chain (poly)sulfides formed will be preferentially deposited on the

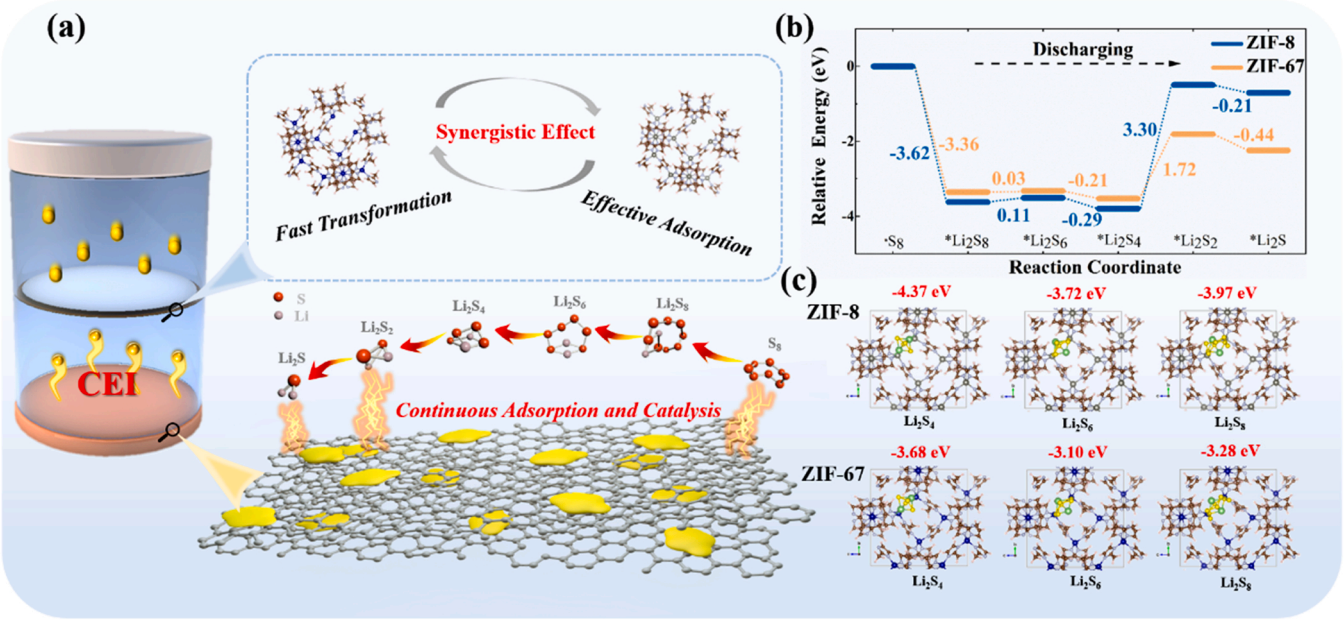

Fig. 1. Reaction mechanism and density functional theory results. (a) Schematic of reaction mechanism of Zn/Co-ZIF nanosheets on polysulfides. (b) Energy profiles for the reduction of LiPSs on ZIF-8 and ZIF-67 substrates. (c) Optimized configurations for the binding of Long-chain Li_2S_n to ZIF-8 and ZIF-67.

conductive cathode host. The directional deposition to the cathode can effectively reduce the (poly)sulfides deposited on the separator modification layer, avoid the loss of active substances, and prevent the active sites of adsorption and catalysis from being occupied, so as to ensure the continuous and effective adsorption and catalysis of (poly)sulfides.

2.2. Materials characterization

A novel simple method for the preparation of Zn/Co-ZIF nanosheets in large quantities is developed, and the yield per unit volume is significantly higher than that of the existing methods (about 200 mg nanosheets can be synthesized in a 50 ml reactor). The Zn/Co-ZIF nanosheets were simply synthesized by a two-step method (Fig. 2a). By pre synthesizing Zn/Co-ZIF nanoparticles (Fig. S4), the ratio of Zn/Co in the subsequent prepared nanosheets can be controlled by adjusting the amount of raw materials. As shown in Fig. 2b, after the hydrothermal reaction and ultrasound treatment, Zn/Co-ZIF nanoparticles were completely exfoliated into Zn/Co-ZIF nanosheets with uniform thickness and size. Compared with the low yield traditional synthesis method, this method can easily realize the preparation of nanosheets in the order of grams. The complete lamellar structure was further confirmed by transmission electron microscope (TEM) image (Fig. 2c) and the single crystal structure of the nanosheet was proved by selected area electron diffraction (SEAD)(Fig. 2d). Through the element mapping of Zn/Co-ZIF nanosheets (Fig. 2e-g) and the spectrum of corresponding elements (Fig. S5), it can be seen that the elements Zn, Co are uniformly distributed, which proves the uniform structure of the nanosheets. In order to further accurately characterize the structural characteristics of the nanosheets, the thickness of the nanosheets was characterized by atomic force microscopy (AFM) (Fig. 3a). The test results show that the thickness of the nanosheets is about 5 nm, and the surface is smooth (Fig. 3b).

The ratios of Zn and Co elements in different ZIF nanosheets are shown in Table S1 and named as ZIF-A, B and C, respectively. By changing the proportion of Zn and Co, there is no obvious difference in the morphology and thickness of the nanosheets (Fig. S6), which can avoid the influence of material morphology and size on its adsorption

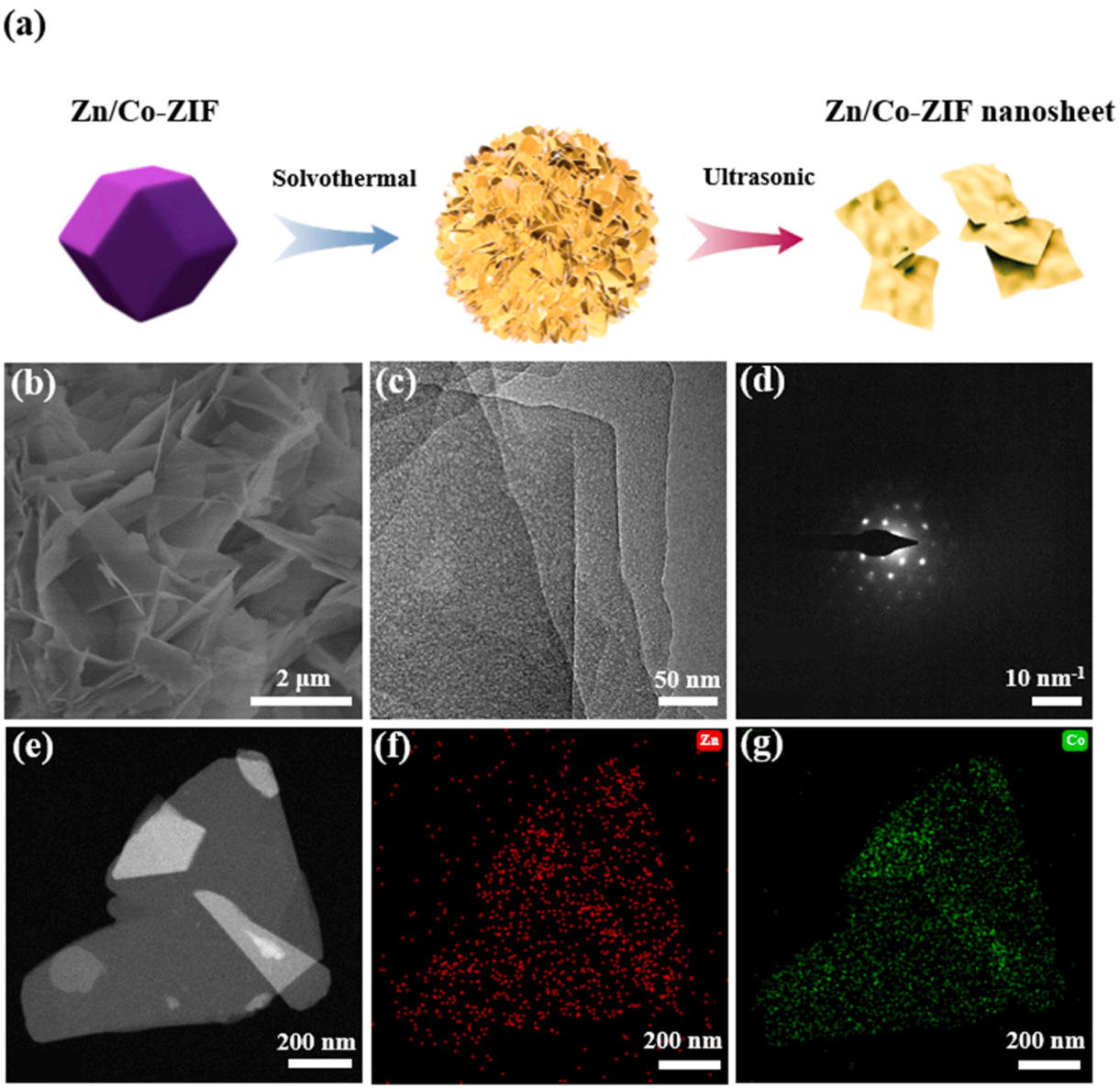

Fig. 2. Schematic of the fabrication of Zn/Co-ZIF nanosheets and the corresponding morphological and structural characterization. (a) Schematic of the fabrication of Zn/Co-ZIF nanosheets. The morphological characterization of Zn/Co-ZIF nanosheets. (b) SEM image. (c) TEM image; (d) SAED pattern and (e-g) TEM elemental mapping images.

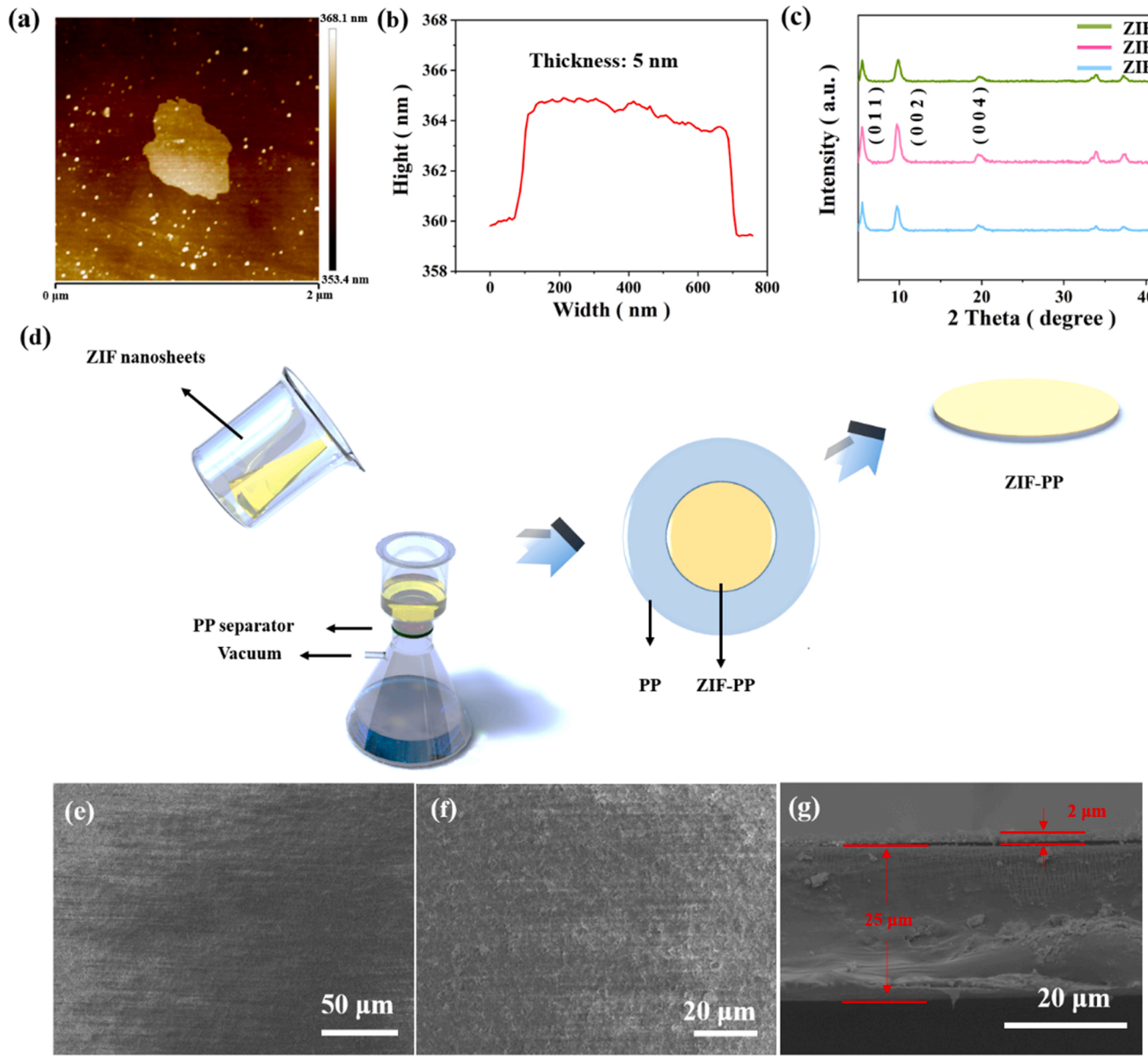

Fig. 3. (a) The AFM image of Zn/Co-ZIF nanosheets and (b) the corresponding thickness variation curve. (c) The XRD patterns of Zn/Co-ZIF nanosheets. (d) Schematic of the preparation of the Zn/Co-ZIF@PP separator. (e,f) SEM image of the surface and (g) the cross-sectional SEM image of Zn/Co-ZIF@PP separator.

and catalysis properties. However, from the optical pictures of the different samples, it can be seen that with the increase of the proportion of Zn, the color of the samples gradually changes from light brown yellow to dark brown yellow (Fig. S7). The X-ray diffractometer (XRD) pattern of the three kinds of nanosheets with different Zn/Co ratios show obvious characteristic peaks of ZIF (Fig. 3c).

2.3. Separator characterization

The prepared nanosheets were redispersed in anhydrous ethanol by ultrasound to form a uniform dispersion. The PP separator was used as a filter membrane, and the nanosheets were modified on the PP separator by vacuum filtration to form Zn/Co-ZIF@PP separator (Fig. 3d). As shown in Fig. 3e, the nanosheets form a very uniform and flat coating layer on the surface of the PP separator. Further, from the higher magnification SEM image (Fig. 3f), it can be seen that the nanosheets are arranged closely and densely. Compared with PP separator, the micro sized pores are completely covered. It also can be seen from the cross-sectional SEM image of the Zn/Co-ZIF@PP separator that a uniform modified layer with a thickness of about 2 μm was formed in the separator (Fig. 3g). The corresponding areal loading of the modification layer is only 0.1 mg cm^{-2}, which is only about one tenth of that of PP separator (1.4 mg cm^{-2}), so it has little influence on the overall area mass of the whole separator. At the same time, compared with the existing work about MOF applied in the separator of Li-S battery, it shows significant advantages in thickness and loadings (Fig. S8). From the optical pictures of Zn/Co-ZIF@PP separator, it can be seen that the surface of the modification separator is light yellow (Fig. S9a). In order to verify the structural stability of the modification layer, we folded and curled the Zn/Co-ZIF@PP separator for many times, and found that the modification layer did not break or fall off from the surface of the PP separator (Fig. S9b-d), which also proved that the modification layer was in close contact with the PP separator, and the structure was very stable. The mechanical properties of Zn/Co-ZIF@PP separator were further confirmed by tensile test. As show in Fig. S10, the maximum load of the Zn/Co-ZIF@PP separator is up to 99.6 MPa, while that of the PP separator is only 24.1 MPa. As a result, the Zn/Co-ZIF@PP separator shows better tensile resistance, which also proves that the mechanical

properties of the modified separator are significantly improved. As we know, the wettability of the separator to the electrolyte affects the ion transfer efficiency, while the traditional PP separator possesses poor wettability to the electrolyte. The dynamic contact angle test shows that Zn/Co-ZIF@PP separator possess excellent wettability for electrolyte. The electrolyte can be completely spread on the surface as soon as it drips down (Fig. S11a), while the electrolyte keeps a certain contact angle on the surface of PP separator, and no diffusion occurred in 30 s (Fig. S11b). The battery will inevitably generate heat during the cycling, so the heat resistance of the separator is also a key factor. The thermal resistance of the separator is observed by recording the temperature change of the separator surface when heated on a heater to 120 ℃ with a thermal imaging camera. As shown in Fig. S12, compared with PP separator, the surface temperature of Zn/Co-ZIF separator is significantly lower, and it is more obvious at higher temperatures. This result also shows that the surface heat conduction of Zn/Co-ZIF separator is slower, so it possesses better heat resistance. The physical and chemical trapping effect of ZIF nanosheets modificaiton layer on polysulfide was also confirmed by permeation test with a double-L device. As shown in Fig. S13, the Li_2S_6 solution and blank electrolyte were separated by the different separators. For the device with PP separator, serious infiltration of Li_2S_6 solution has occurred in about 6 h and almost completely after 48 h. In contrast, the device with Zn/Co-ZIF@PP separator shows only a small amount of polysulfide penetration even after 48 h, which also proves the compactness of ZIF nanosheets modification layer and strong physical and chemical restriction on polysulfide.

2.4. Electrochemical performance

In order to explore the role of Zn and Co metal center sites in the nanosheets for (poly)sulfides, the three kinds of nanosheets with different Zn and Co contents were applied for separator modification, and assembled batteries with the freestanding S/rGO composite cathode to test the relevant electrochemical performance. The areal sulfur loading of the cathode for routine electrochemical performance test is 2.1 mg cm^{-2}. Fig. 4a were the typical cyclic voltammetry (CV) profiles for the Li-S battery assembled with different separators. With the ZIF-B modified separator, the two cathodic peaks at 2.30 V and 2.06 V are attributed to the reduction of soluble (poly)sulfides (Li_2S_x, $3 < x \leq 8$) and the formation of solid Li_2S_2 and Li_2S, respectively. The Li-S battery also shows an obvious anodic peak at 2.36 V, which is lower than that of

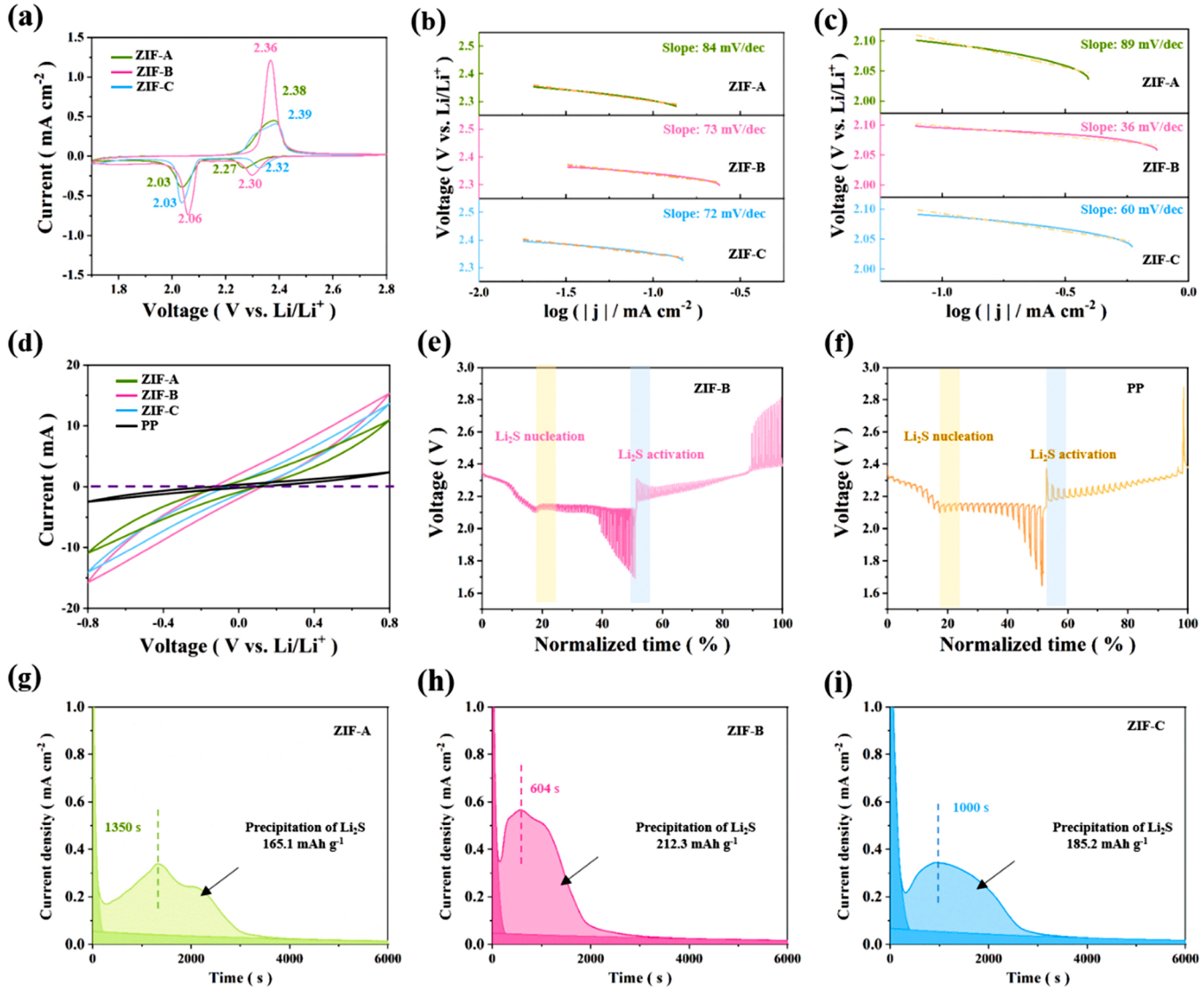

Fig. 4. Catalytic performance of the Li-S cell with different ZIF nanosheets modified separator. (a) CV curves; (b,c) Tafel slopes from the cathodic peaks of the CV curves. (d) CV curves of symmetric cells at 30 mV S^{-1}. The GITT plots of Li-S batteries with (e) ZIF-B@PP separator and (f) PP separator in the first discharge/charge process under the current density of 0.05 C. Chronoamperometric curves of nucleation tests using (g) ZIF-A, (h) ZIF-B and (i) ZIF-C.

the Li-S battery assembled with ZIF-A (2.38 V) and ZIF-C (2.39 V). The Tafel slopes of the Li-S battery assembled with three different separators derived from the two cathodic peaks are shown in Fig. 4b,c. By fitting the cathodic peak corresponding to the transformation of long-chain (poly)sulfides, the ZIF-B and ZIF-C modified separators show the lower Tafel slope. As for the cathodic peak corresponding to the transformation of Li_2S_2 and Li_2S, the Tafel slope of ZIF-B (36 mV/dec) modified separator is significantly lower than that of the ZIF-A (89 mV/dec) and ZIF-C (60 mV/dec) modified separators, which is due to the synergistic effect of Zn and Co metal center. This difference is more obvious at higher scan rate, which also proves the fast reaction kinetics in the cell assembled with ZIF-B modified separator. In order to further prove the effectiveness of different nanosheets in catalyzing the conversion of (poly)sulfides, we assembled the symmetrical battery with Li_2S_6. As shown in Fig. 4d, the current responses of Zn/Co-ZIF@PP symmetrical cells are much higher than that of PP separator, especially the ZIF-B. The Galvanostatic intermittent titration technique (GITT) measurements were employed to study the nucleation and activation process of Li_2S. Obviously, the ZIF-B@PP separator (Fig. 4e) delivered lower discharge/charge polarization voltage plateaus when compared with the PP cell (Fig. 4f). It is further proved that ZIF-B@PP separator facilitates the redox reaction of (poly)sulfides. In the same voltage range, more cycles can be carried out with ZIF-B@PP separator assembled, which also proves that it can effectively inhibit the self-discharge effect of Li-S battery. The electrochemical impedance spectroscopic (EIS) tests of Li-S battery with different separators are shown in Fig. S14. The EIS curves show that the ZIF-B exhibits the smallest charge transfer resistance, implying its fast charge transfer kinetics at the interface. In order to further verify the effect of different ZIFs on the precipitation of Li_2S. Fig. 4g-i show the current curves corresponding to the reduction of Li_2S_8/Li_2S_6 and the precipitation of Li_2S for different ZIFs [39,40]. Rapid current changes were shown with ZIF-B (604 s) and ZIF-C (1000 s), which is attributed to the catalytic effect of Co cites on (poly)sulfides. More importantly, the precipitation capacity of Li_2S with ZIF-B based battery is 212.3 mAh g^{-1}, which is higher than that of ZIF-A (165.1 mAh g^{-1}) and ZIF-C (185.2 mAh g^{-1}) based batteries.This result is due to the continuous balanced adsorption and catalysis of Zn and Co centers on (poly)sulfides, which well verifies the calculation results.

The electrochemical performances of Li-S batteries with different separators at 0.5 C are shown in Fig. 5a. Thanks to the high catalytic activity of Co metal cites, the ZIF-C possess faster reaction kinetics than ZIF-A, so it shows higher capacity in the initial stage. After several cycles of activation, the ZIF-A shows a more stable cycle, which is mainly because Zn metal center has better adsorption effect on (poly)sulfides.

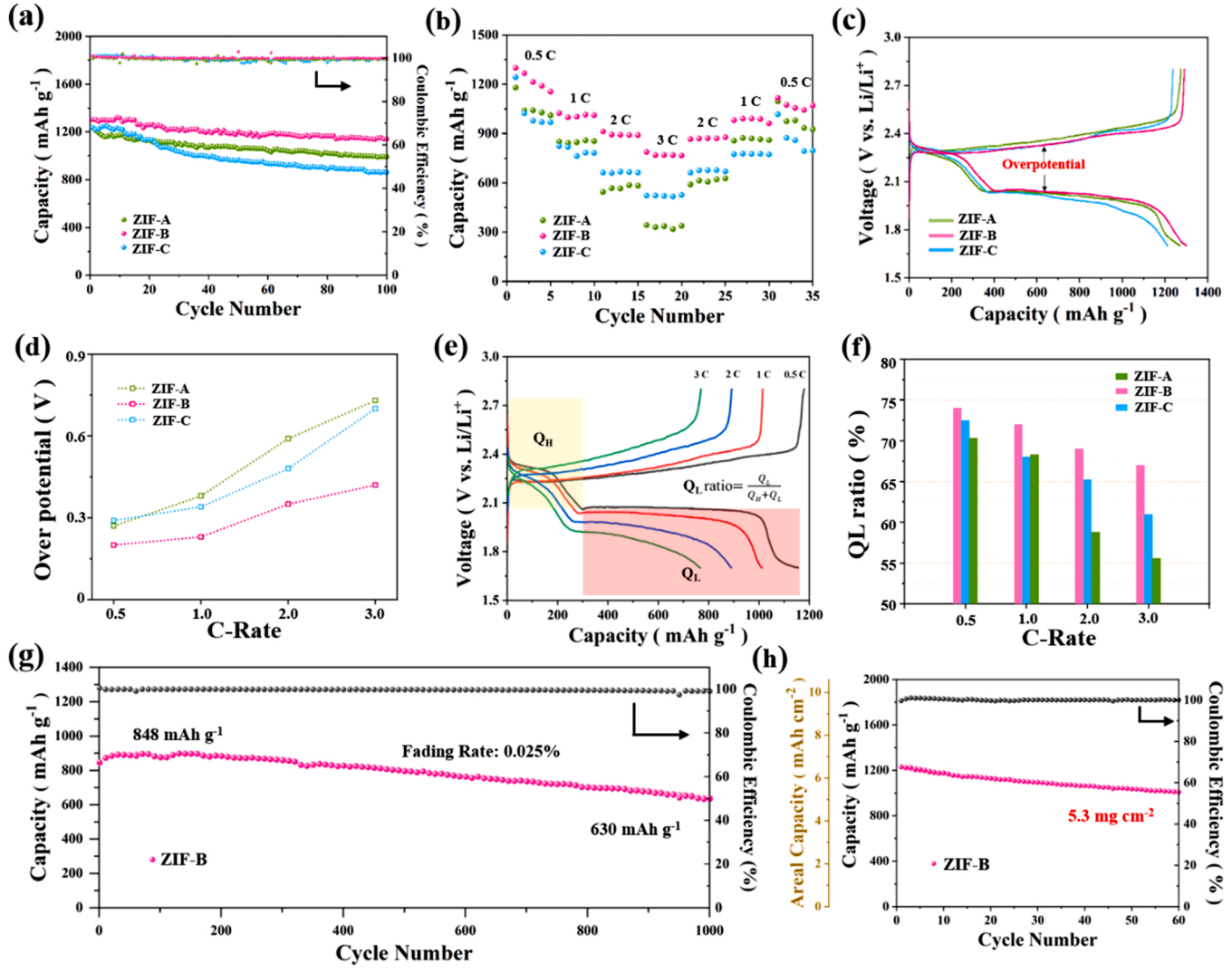

Fig. 5. Electrochemical performance of the Li-S cell with different ZIF nanosheets modified separator. (a) Cycling test at 0.5 C. (b) Rate performance. (c) Galvanostatic charge-discharge profiles at 0.5 C in potential window from 1.7 V to 2.8 V. (d) The over potential at different rates. (e) Galvanostatic charge-discharge profiles of the Li-S cell with ZIF-B@PP separator at different rates. (f) The Q_L ratio at different rates. (g) Long-term performance of ZIF-B@PP separator at a current density of 2 C. (h) Cycling stability under high sulfur loading.

Due to the synergistic effects of Zn and Co in adsorption and catalysis of (poly)sulfides, the ZIF-B@PP separator delivers the highest initial capacity of 1304 mAh g^{-1} and maintained at 1141 mAh g^{-1} after 100 cycles. The rate performance of the battery assembled with different separators was also studied (Fig. 5b). Similarly, the ZIF-B@PP separator shows the highest discharge capacity of 1300, 1024, 912 and 788 mAh g^{-1} at 0.5, 1, 2 and 3 C, respectively. Since faster polysulfide oxidation and reduction are required at high rate, the ZIF-C with higher Co content possesses higher reversible capacity than ZIF-A at high current density of 3 C. In addition, the ZIF-B@PP separator also exhibit the lowest polarization potential at 0.5 C (Fig. 5c). However, with the increase of current density, the polarization voltages of ZIF-C@PP and ZIF-A@PP separator increase significantly. At a high rate of 3 C, the polarization voltages of ZIF-C@PP (0.70 V) and ZIF-A@PP (0.73 V) separators are much higher than that of ZIF-B@PP separator (0.42 V) (Fig. 5d). As we know, the discharge plateau around 2.1 V is corresponding to the transformation of Li_2S_4 to Li_2S, so the theoretical capacity (Q_L) is 75% of the total capacity (Fig. 5e). For comparison, the constant current charge/discharge voltage curves of different rate for Li-S batteries assembled with different separators are shown Fig. S15. As for the ZIF-C@PP and ZIF-A@PP separator, the Q_L ratio decreases severely from 0.5 C to 3 C, showing lower ratios of 61% and 56% at 3 C, respectively (Fig. 5 f). On the other hand, the ZIF-B@PP separator exhibit a high Q_L ratio of 74% at 0.5 C, even at 3 C, the Q_L ratio can be maintained at 67%. The results also indicate that the ZIF-B is more conducive to promote the conversion reaction of soluble Li_2S_X species to solid Li_2S than ZIF-C and ZIF-A. Fig. 5 g is the long-term cycle performance of Li-S battery assembled with ZIF-B@PP separator at 2 C. The battery shows a high initial capacity of 848 mAh g^{-1}. After 1000 cycles, the capacity is maintained about 630 mAh g^{-1}, and the corresponding fading rate is only 0.025% per cycle. As we know, the areal loading of sulfur in the cathode affects the commercial application of the Li-S battery. Therefore, it is of great significance to test the performance of the separator under high sulfur loadings. As shown in Fig. 5 h, even with a high sulfur loading of 5.3 mg cm^{-2}, the Li-S cell assembled with ZIF-B@PP separator shows a high initial capacity of 1227 mAh g^{-1} (6.5 mAh cm^{-2}) at 0.2 C, and maintained at 1007 mAh g^{-1} (5.3 mAh cm^{-2}) after 60 cycles. As shown in Fig. S16, the structure of the separator modification layer can still remain intact, which also proves that the modification layer can provide continuous conversion of polysulfides. In summary, owing to the synergistic effect of Zn and Co metal cites, the Li-S cell assembled with ZIF-B shows the best electrochemical performance under different test conditions. And compared with other work based on MOF separator in Li-S battery (Table S2), this work possceses great advantages in the loading of modification layer, rate performance and cycle stability.

3. Conclusion

In conclusion, we systematically investigated the effects of adsorption and catalysis of (poly)sulfides with the separator modification layer on the performance of Li-S battery. The 2D-Zn/Co-ZIF nanosheets with different Zn/Co ratio prepared by a novel method were used as the research object. Combined with a variety of tests, the different adsorption or catalysis effects of Zn/Co metal centers on (poly)sulfides were verified. Based on the difference in conductivity of the ZIF modification layer and the cathode, a continuous adsorption and catalysis of (poly) sulfides were realized between the cathode electrolyte interface by the separator modification layer. The final results show that the Li-S battery assembled with the ZIF-B@PP separator possess better electrochemical properties. With this functional separator, the Li-S battery can deliver a high initial capacity of 1304 mAh g^{-1} at 0.5 C and achieve a reversible capacity of 788 mAh g^{-1} at 3 C. The battery also show a lower capacity fading rate of 0.025% at 2 C over 1000 cycles. Even with a high sulfur loading of 5.3 mg cm^{-2}, the Li-S battery provide a high initial areal capacity of 6.5 mAh cm^{-2}. Therefore, this work will provide a new way for the preparation of 2D-ZIF nanosheets in large-scale, and has important guiding significance for exploring the adsorption and catalysis effect of MOF metal centers for (poly)sulfides.

CRediT authorship contribution statement

C. Zhou and **M.J. Chen** contributed equally to this work. **C. Zhou** designed the experiments and performed the data analyses as well as wrote the manuscript. **M.J. Chen and C.X. Dong** carried out synthesis. **H. Wang and C.L. Shen** carried out TEM abalysis and draw the schematic diagram. **X.X. Wu and Q.Y. An** contributed to the conception of the study and revised the manuscript. **G.G. Chang, X. Xu and L.Q. Mai** were in charge of this scientific research project, and the leaders of actual coordination of contributions.

Declaration of Competing Interest

The authors declare that they have no known competing financial interests or personal relationships that could have appeared to influence the work reported in this paper.

Acknowledgements

This work was supported by China-Japanese Research Cooperative Program founded by the Ministry of Science and Technology of the People's Republic of China (2017YFE0127600), the National Natural Science Foundation of China (52127816, 51872218), the Young Top-notch Talent Cultivation Program of Hubei Province, and the Fundamental Research Funds for the Central Universities (WUT: 2020III023, 2020III050, 2021IVA123, 2021III009), the National innovation and entrepreneurship training propram for college students (No. S202110497006), and Sanya Science and Education Innovation Park of Wuhan University of Technology (2020KF0021) (all the laboratories are at WUT). The authors thank Dr. Congli Sun of Nanostructure Research Center (NRC) at WUT for the TEM test.

Appendix A. Supporting information

Supplementary data associated with this article can be found in the online version at doi:10.1016/j.nanoen.2022.107332.

References

[1] A. Manthiram, S.H. Chung, C.X. Zu, Lithium-sulfur batteries: progress and prospects, Adv. Mater. 27 (2015) 1980–2006.
[2] A. Manthiram, Y.Z. Fu, Y.S. Su, Challenges and prospects of lithium-sulfur batteries, Acc. Chem. Res. 46 (2013) 1125–1134.
[3] Z.W. Seh, Y.M. Sun, Q.F. Zhang, Y. Cui, Designing high-energy lithium-sulfur batteries, Chem. Soc. Rev. 45 (2016) 5605–5634.
[4] A. Manthiram, Y.Z. Fu, S.H. Chung, C.X. Zu, Y.S. Su, Rechargeable lithium-sulfur batteries, Chem. Rev. 114 (2014) 11751–11787.
[5] M. Zhao, B.Q. Li, X.Q. Zhang, J.Q. Huang, Q. Zhang, A. Perspective, Perspective toward practical lithium-sulfur batteries, ACS Cent. Sci. 6 (2020) 1095–1104.
[6] P. Bonnick, J. Muldoon, The Dr Jekyll and Mr Hyde of lithium sulfur batteries, Energy Environ. Sci. 13 (2020) 4808–4833.
[7] X. Chen, T.Z. Hou, K.A. Persson, Q. Zhang, Combining theory and experiment in lithium-sulfur batteries: Current progress and future perspectives, Mater. Today 22 (2019) 142–158.
[8] T.Y. Pan, Z.H. Li, Q. He, X. Xu, L. He, J.S. Meng, C. Zhou, Y. Zhao, L.Q. Mai, Uniform zeolitic imidazolate framework coating via in situ recoordination for efficient polysulfide trapping, Energy Storage Mater. 23 (2019) 55–61.
[9] X.W. Liu, Z.H. Li, X.B. Liao, X.F. Hong, Y. Li, C. Zhou, Y. Zhao, X. Xu, L.Q. Mai, A three-dimensional nitrogen-doped graphene framework decorated with an atomic layer deposited ultrathin V_2O_5 layer for lithium sulfur batteries with high sulfur loading, J. Mater. Chem. A 8 (2020) 12106–12113.
[10] Z.H. Li, Q. He, X. Xu, Y. Zhao, X.W. Liu, C. Zhou, D. Ai, L.X. Xia, L.Q. Mai, A 3D nitrogen-doped graphene/TiN nanowires composite as a strong polysulfide anchor for lithium-sulfur batteries with enhanced rate performance and high areal capacity, Adv. Mater. 30 (2018), 1804089.
[11] B.R. Liu, M. Taheri, J.F. Torres, Z. Fusco, T. Lu, Y. Liu, T. Tsuzuki, G.H. Yu, A. Tricoli, Janus conductive/insulating microporous ion-sieving membranes for stable Li-S batteries, ACS Nano 14 (2020) 13852–13864.
[12] X.Z. Huang, R. He, M. Li, M.O.L. Chee, P. Dong, J. Lu, Functionalized separator for next-generation batteries, Mater. Today 41 (2020) 143–155.

[13] Z.H. Li, C. Zhou, J.H. Hua, X.F. Hong, C.L. Sun, H.W. Li, X. Xu, L.Q. Mai, Engineering oxygen vacancies in a polysulfide-blocking layer with enhanced catalytic ability, Adv. Mater. 32 (2020), 1907444.
[14] J.R. He, Y.F. Chen, A. Manthiram, Vertical Co_9S_8 hollow nanowall arrays grown on a Celgard separator as a multifunctional polysulfide barrier for high-performance Li-S batteries, Energy Environ. Sci. 11 (2018) 2560–2568.
[15] Z.J. Zheng, H. Ye, Z.P. Guo, Recent progress on pristine metal/covalent-organic frameworks and their composites for lithium-sulfur batteries, Energy Environ. Sci. 14 (2021) 1835–1853.
[16] S.R. Luo, F.X. Wu, G. Yushin, Strategies for fabrication, confinement and performance boost of Li_2S in lithium-sulfur, silicon-sulfur & related batteries, Mater. Today 49 (2021) 253–270.
[17] Z. Chang, Y. Qiao, J. Wang, H. Deng, P. He, H.S. Zhou, Fabricating better metal-organic frameworks separators for Li-S batteries: pore sizes effects inspired channel modification strategy, Energy Storage Mater. 25 (2020) 164–171.
[18] Y.J. Li, T.T. Gao, D.Y. Ni, Y. Zhou, M. Yousaf, Z.Q. Guo, J.H. Zhou, P. Zhou, Q. Wang, S.J. Guo, Two Birds with One Stone: Interfacial Engineering of Multifunctional Janus Separator for Lithium-Sulfur Batteries, Adv. Mater. 34 (2022) 2107638.
[19] M.T. Liu, S. Jhulki, Z.F. Sun, A. Magasinski, C. Hendrix, G. Yushin, Atom-economic synthesis of Magneli phase Ti_4O_7 microspheres for improved sulfur cathodes for Li-S batteries, Nano Energy 79 (2021), 105428.
[20] Q.P. Wu, Z.G. Yao, X.J. Zhou, J. Xu, F.H. Cao, C.L. Li, Built-In catalysis in confined nanoreactors for high-loading Li-S batteries, ACS Nano 14 (2020) 3365–3377.
[21] R.R. Li, H.J. Peng, Q.P. Wu, X.J. Zhou, J. He, H.J. Shen, M.H. Yang, C.L. Li, Sandwich-like Catalyst-Carbon-Catalyst Trilayer Structure as a Compact 2D Host for Highly Stable Lithium-Sulfur Batteries. Angewandte Chemie International Edition, Wiley, 2020, pp. 12129–12138.
[22] Z. Zhang, D. Luo, G.R. Li, R. Gao, M. Li, S. Li, L. Zhao, H.Z. Dou, G.B. Wen, S. Sy, Y. F. Hu, J.D. Li, A.P. Yu, Z.W. Chen, Tantalum-based electrocatalyst for polysulfide catalysis and retention for high-performance lithium-sulfur batteries, Matter 3 (2020) 920–934.
[23] Z.F. Liang, D.W. Yang, P.Y. Tang, C.Q. Zhang, J.J. Biendicho, Y. Zhang, J. Llorca, X. Wang, J.S. Li, M. Heggen, J. David, R.E. Dunin-Borkowski, Y.T. Zhou, J. R. Morante, A. Cabot, J. Arbiol, Atomically dispersed Fe in a C_2N based catalyst as a sulfur host for efficient lithium-sulfur batteries, Adv. Energy Mater. 11 (2021), 2003507.
[24] X. Zhou, P. Zeng, H. Yu, C.M. Guo, C.Q. Miao, X.W. Guo, M.F. Chen, X.Y. Wang, ACS Appl. Mater. Interfaces 14 (2022) 1157–1168.
[25] M.F. Chen, S. Zhao, S.X. Jiang, C. Huang, X.Y. Wang, Z.H. Wang, K.X. Xiang, Y. Zhang, Suppressing the polysulfide shuttle effect by heteroatom-doping for high-performance lithium–sulfur batteries, ACS Sustain. Chem. Eng. 6 (2018) 7545–7557.
[26] B. Guan, Y. Zhang, L.S. Fan, X. Wu, M.X. Wang, Y. Qiu, N.Q. Zhang, K.N. Sun, Blocking polysulfide with Co_2B@CNT via "synergetic adsorptive effect" toward ultrahigh-rate capability and robust lithium-sulfur battery, ACS Nano 13 (2019) 6742–6750.
[27] Z.B. Cheng, H. Pan, J.Q. Chen, X.P. Meng, R.H. Wang, Separator modified by cobalt-embedded carbon nanosheets enabling chemisorption and catalytic effects of polysulfides for high-energy-density lithium-sulfur batteries, Adv. Energy Mater. 9 (2019), 1901609.
[28] C. Zhou, Q. He, Z.H. Li, J.S. Meng, X.F. Hong, Y. Li, Y. Zhao, X. Xu, L.Q. Mai, A robust electrospun separator modified with in situ grown metal-organic frameworks for lithium-sulfur batteries, Chem. Eng. J. 395 (2020), 124979.
[29] Y.J. Li, S.Y. Lin, D.D. Wang, T.T. Gao, J.W. Song, P. Zhou, Z.K. Xu, Z.H. Yang, N. Xiao, S.J. Guo, Single atom array mimic on ultrathin MOF nanosheets boosts the safety and life of lithium-sulfur batteries, Adv. Mater. 32 (2020), 1906722.
[30] S.Y. Bai, X.Z. Liu, K. Zhu, S.C. Wu, H.S. Zhou, Metal-organic framework-based separator for lithium-sulfur batteries, Nat. Energy 1 (2016) 16094.
[31] M. Tian, F. Pei, M.S. Yao, Z.H. Fu, L.L. Lin, G.D. Wu, G. Xu, H. Kitagawa, X.L. Fang, Ultrathin MOF nanosheet assembled highly oriented microporous membrane as an interlayer for lithium-sulfur batteries, Energy Storage Mater. 21 (2019) 14–21.
[32] Z.Q. Wang, W.Y. Huang, J.C. Hua, Y.D. Wang, H.C. Yi, W.G. Zhao, Q.H. Zhao, H. Jia, B. Fei, F. Pan, An anionic-MOF-based bifunctional separator for regulating lithium deposition and suppressing polysulfides shuttle in Li-S batteries, Small Methods 4 (2020), 2000082.
[33] A.E. Baumann, X. Han, M.M. Butala, V.S. Thoi, Lithium thiophosphate functionalized zirconium MOFs for Li-S batteries with enhanced rate capabilities, J. Am. Chem. Soc. 141 (2019) 17891–17899.
[34] D. Luo, C.J. Li, Y.G. Zhang, Q.Y. Ma, C.Y. Ma, Y.H. Nie, M. Li, X.F. Weng, R. Huang, Y. Zhao, L.L. Shui, X. Wang, Z.W. Chen, Design of Quasi-MOF Nanospheres as a Dynamic Electrocatalyst toward Accelerated Sulfur Reduction Reaction for High-Performance Lithium-Sulfur Batteries, Adv. Mater. 34 (2022) 2105541.
[35] P.B. Geng, L. Wang, M. Du, Y. Bai, W.T. Li, Y.F. Liu, S.Q. Chen, P. Braunstein, Q. Xu, H. Pang, MIL-96-Al for Li-S Batteries: Shape or Size? Adv. Mater. 34 (2022) 2107836.
[36] J.W. Zhou, R. Li, X.X. Fan, Y.F. Chen, R.D. Han, W. Li, J. Zheng, B. Wang, X.G. Li, Rational design of a metal-organic framework host for sulfur storage in fast, long-cycle Li-S batteries, Energy Environ. Sci. 7 (2014) 2715–2724.
[37] C. Zhou, Z. Li, X. Xu, L. Mai, Metal-organic frameworks enable broad strategies for lithium-sulfur batteries, Natl. Sci. Rev. 8 (2021) nwab055.
[38] H. Wang, F. Liu, R. Yu, J. Wu, Unraveling the reaction mechanisms of electrode materials for sodium-ion and potassium-ion batteries by in situ transmission electron microscopy, Interdiscip. Mater. 1 (2022) 196–212.
[39] F.Y. Fan, W.C. Carter, Y.M. Chiang, Mechanism and kinetics of Li_2S precipitation in lithium-sulfur batteries, Adv. Mater. 27 (2015) 5203–5209.
[40] C. Zhao, G.L. Xu, Z. Yu, L.C. Zhang, I. Hwang, Y.X. Mo, Y.X. Ren, L. Cheng, C. J. Sun, Y. Ren, X.B. Zuo, J.T. Li, S.G. Sun, K. Amine, T.S. Zhao, A high-energy and long-cycling lithium-sulfur pouch cell via a macroporous catalytic cathode with double-end binding sites, Nat. Nanotechnol. 16 (2021) 166–173.

Cheng Zhou received his B.S. degree from Wuhan University of Science and Technology in 2016 and M.S. degree from Wuhan University of Technology (WUT) in 2019. He is currently a Ph.D. candidate in Materials Science and Engineering at WUT. His current research focuses on developing novel nanomaterials and structures for lithium metal batteries.

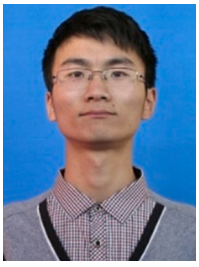

Minjie Chen received his B.S. degree from WUT majoring in Chemical Engineering and Technology in 2019. He is currently a M.S. degree candidate under the supervision of Prof. Gang-Gang Chang at WUT. His main research interests are the synthesis of two-dimensional MOF and its derivatives for heterogeneous catalysis.

Chenxu Dong is currently working toward the B.S. degree in Materials Science and Engineering from WUT. His current research focus on the synthesis and characterization of advanced materials for Li-S batteries.

Hong Wang obtained her M. S. degree in Physical Chemistry from Wuhan University in 2013. She had worked as a teacher in School of Mathematics and Physics, Jingchu University of Technology (2014–2019). She is currently working toward the Ph.D. degree in Materials Science and Engineering at WUT. Her current research focuses on in-situ transmission electron microscopy and scanning transmission electron microscopy and their applications in energy storage materials.

Chunli Shen is currently a Ph.D student in the State Key Laboratory of Advanced Technology for Materials Synthesis and Processing at WUT. Her research focuses on the Li metal batteries and solid-state electrolytes.

Ganggang Chang received his Ph.D. degree (2016) in applied chemistry from Zhejiang University under the direction of Prof. Qilong Ren, and joined Prof. Banglin Chen's group as a visiting scholar at the University of Texas at San Antonio during 2015–2016. Now he is working at WUT as an associate professor in the School of Chemistry, Chemical Engineering and Life Science. His current research interests are hierarchically porous materials for catalysis and separation application.

Xiuxiu Wu received her B.S. degree from Qingdao University of Science and Technology majoring in Material Science and Technology in 2019. She is currently a Master degree candidate under the supervision of Dr. Xu Xu at WUT. Her main research interests are the separator modification of Lithium-sulfur battery.

Xu Xu is an Associate Professor in the International School of Materials Science and Engineering at WUT. He received his Ph. D. degree in Materials Science from WUT, and worked as a visiting graduate researcher at University of California, Los Angeles. His current research interests mainly focus on energy storage materials and devices, including lithium sulfur battery, lithium metal battery and thin film battery.

Qinyou An is Professor of Materials Science and Engineering at WUT. He received his Ph.D. degree from WUT in 2014. He carried out his postdoctoral research in the laboratory of Prof. Yan Yao at the University of Houston in 2014–2015. Currently, his research interest includes energy storage materials and devices.

Liqiang Mai is the Chair professor of Materials Science and Engineering at WUT, Dean of School of Materials Science and Engineering at WUT, Fellow of the Royal Society of Chemistry. He received his Ph.D. from WUT in 2004 and carried out his postdoctoral research at Georgia Institute of Technology in 2006–2007. He worked as an advanced research scholar at Harvard University and University of California, Berkeley. His current research interests focus on new nanomaterials for electrochemical energy storage and micro/nano energy devices.